Interplays between copper and *Mycobacterium tuberculosis* GroEL1

Dong Yang [1], David P. Klebl [2, 3], Sheng Zeng [1], Frank Sobott [2, 4, 5], Martine Prévost [6], Patrice Soumillion [7], Guy Vandenbussche [6 #] and Véronique Fontaine [1, #,*]

[1] Microbiology, Bioorganic and Macromolecular Chemistry Unit, Faculty of Pharmacy, Université Libre de Bruxelles (ULB), Brussels, Belgium

[2] The Astbury Centre for Structural Molecular Biology, University of Leeds, Leeds, UK

[3] School of Biomedical Sciences, University of Leeds, Leeds LS2 9JT, UK

[4] School of Molecular and Cellular Biology, University of Leeds, Leeds LS2 9JT, UK

[5] BAMS Research Group, Department of Chemistry, University of Antwerp, Antwerp, 2020, Belgium

[6] Laboratory for the Structure and Function of Biological Membranes, Faculty of Sciences, Université Libre de Bruxelles (ULB), Brussels, Belgium

[7] Biochemistry and Genetics of Microorganisms, Louvain Institute of Biomolecular Science and Technology, Université Catholique de Louvain (UCL), Louvain-la-Neuve, Belgium

[#] Equally contributed

* Corresponding author, email: vfontain@ulb.ac.be, postal address: Microbiology, Bioorganic and Macromolecular Chemistry Unit, Faculty of Pharmacy, Université Libre de Bruxelles (ULB), Boulevard du Triomphe, CP205/2, 1050 Brussels, Belgium

Abstract

The recalcitrance of pathogenic *Mycobacterium tuberculosis*, the agent of tuberculosis, to eradication is due to various factors allowing bacteria to escape from stress situations. The mycobacterial chaperone GroEL1, overproduced after macrophage entry and under oxidative stress, could be one of these key players. Indeed, GroEL1 was shown to be necessary for the virulent phthiocerol dimycocerosate lipid biosynthesis and for various types of drug resistance. In the present study, we observed that GroEL1, having a unique C-terminal histidine-rich region, is required for copper tolerance during *Mycobacterium bovis* BCG biofilm development. Mass spectrometry analysis demonstrated that GroEL1 displays high affinity for copper ions, especially at its C-terminal histidine-rich region. Furthermore, the binding of copper protects GroEL1 from destabilization and increases GroEL1 ATPase activity. Altogether, these findings suggest that GroEL1 could counteract copper toxicity, notably in the macrophage phagosome, and further emphasizes that the *M. tuberculosis* GroEL1 could be an interesting antitubercular target.

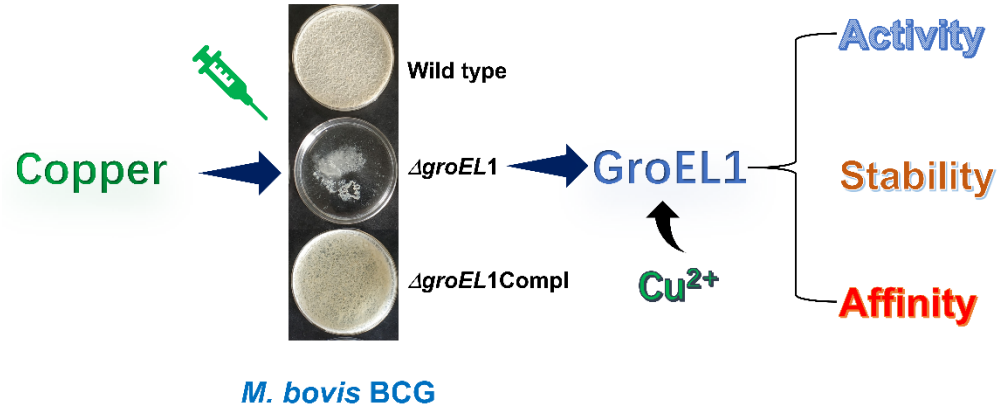

Mycobacteria chaperone GroEL1 enhances copper tolerance during *Mycobacterium bovis* BCG biofilm formation. Copper ion strongly binds to GroEL1 natural histidine-rich region protecting GroEL1 from destabilization and increasing GroEL1 ATPase activity.

Introduction

Mycobacterium tuberculosis is the causative agent of tuberculosis (TB), a leading infectious disease still causing an estimated 10 million TB cases and 1.4 million deaths in 2018 [1]. This bacterial infection is difficult to treat for various reasons. First, the bacterium has an unusual impermeable cell wall reducing drug accessibility. This cell wall is composed, from the inside to the outside, of peptidoglycan covalently bound to arabinogalactan which in turn can also be covalently bound to exceptionally long chain fatty acids, mycolic acids. Those are further embedded in an outer membrane, rich in non-covalently bound long fatty acids [2, 3]. Among the non-covalently embedded lipids, phthiocerol dimycocerosates (PDIM), methyl-branched fatty acid-containing lipids, are essential to resist to hostile environment and antibiotics [3-6].

In addition, this pathogen can adopt different strategies to escape bactericidal stress, *e.g.* oxidative stress within macrophages and hypoxia in lung granuloma, among others by entering into a nonreplicating state called dormancy [7-10]. The mycobacterial GroEL1 chaperonin has been previously shown to be essential for metabolic and energetic adaptation under stress, as reflected *in vitro* in a biofilm growth model [11].

M. bovis and *M. tuberculosis* have two *GroEL* encoding genes, *groEL*1 (*Rv3417c*, BCG_*3487c*) in an operonic arrangement with *groES* (*Rv3418c*, BCG_*3488c*) and *groEL*2 (*Rv0440*, BCG_*0479*) [12]. They encode two forms of chaperone proteins, GroEL1 (Cpn60.1, Hsp60.1) and GroEL2 (Cpn60.2, Hsp60.2), which are identical between *M. tuberculosis* and *M. bovis*. GroEL1 shares 62 % sequence identity with GroEL2 [12] and 53 % sequence identity and 70% similarity with the well-known *E. coli* GroEL[13]. The *E. coli* GroEL can oligomerize in two heptameric structures stacked back-to-back to promote protein folding with the help of the cochaperonin GroES, in an ATP-dependent manner [14-18]. The divalent cation Mg^{2+} and to a less extent Mn^{2+}, Co^{2+} or Ni^{2+}, has been shown to be required for the *E. coli* GroEL ATPase activity [19]. Interestingly, *M. tuberculosis* GroEL1 has a distinctive histidine-rich C-terminal region, while GroEL2 has a glycine-methionine-rich C-terminal region that is more typical of these chaperones [12]. In *M. tuberculosis*, both GroEL proteins are overproduced under stress conditions, including heat shock [20], oxidative

stress response [21, 22], osmotic stress [23] and in macrophage infection [24]. The *M. bovis* BCG *groEL*1 knockout mutant shows increased sensitivity to oxidative stress and vancomycin compared to wild type strain [5]. Furthermore, our previous research demonstrated that the GroEL1 chaperone protein is required for PDIM biosynthesis as the *M. bovis* BCG Δ*groEL1* mutant is devoid of PDIM [5]. Usually, under stress, bacteria use a common virulence and adaptive factor to survive, they form biofilms [13, 22, 25, 26]. Although mycobacterial biofilms were not yet observed in patients with tuberculosis, pathologies involving nontuberculous mycobacteria were shown to be associated with biofilm infections. For pathogenic mycobacteria, biofilm has been shown to be an interesting *in vitro* growth model as, in biofilm, mycobacteria are entering into dormancy and develop adaptative bactericidal escape mechanisms like in *in vivo* stress conditions [27]. For mycobacterial biofilm formation, high concentration of glycerol (6 % of culture medium) are used and GroEL1 was shown to be required to adapt to this high glycerol concentration [11]. In *in vivo* stress conditions, such as in the phagosome macrophage compartment and in the lungs, mycobacteria encounter increased metal ion concentrations [28-30]. Although copper is essential for mycobacteria viability, the high copper ion concentration in host/cell compartments is an efficient antibacterial defence mechanism, especially against the susceptible *M. tuberculosis* [31-33].

The specific GroEL1 C-terminal histidine-rich region has been predicted to be involved in metal binding [12]. This was confirmed in the purification process of *M. smegmatis* GroEL1 using Ni-agarose affinity matrix and more recently by isothermal titration calorimetry (ITC) [13, 34]. Given the overproduction of GroEL1 under stress, we evaluated *M. bovis* BCG biofilm growth in the presence of metal ions and further investigated the impact of metal ions on GroEL1 biochemical characteristics.

Experimental section

Bacterial strains and growth condition

M. bovis BCG GL2 strains, wild type (wt), BCG Δ*groEL*1 (KO) and BCG complemented (compl) have been described previously [22]. *M. bovis* BCG strains were precultured in Middlebrook 7H9 medium (Difco Laboratories) containing 0.05% Tween 80 supplemented with 10% albumin-dextrose complex. BCG Δ*groEL*1 (KO) preculture contained 25 μg/mL kanamycin, BCG complemented (compl) preculture contained 25 μg/mL kanamycin and 50 μg/mL hygromycin.

M. bovis BCG biofilm formation

The biofilm cultures were grown on modified Sauton's medium containing 3.5% (v/v) glycerol in the presence or absence of Cu^{2+}, Zn^{2+} or Cd^{2+}. One litre of Sauton's medium contains 0.5 g KH_2PO_4, 0.5 g $MgSO_4$, 2.0 g citric acid, 0.05 g ferric ammonium citrate, 35 mL glycerol, 4.0 g asparagine, 1.435 mg $ZnSO_4$ and is adjusted to pH 7.2 with 1 M NaOH.

Briefly, 20 μL or 100 μL of preculture (OD_{600} at 0.9-1.0) were inoculated in 2 mL or 10 mL biofilm medium (in a well of a 24-well plate or in a 6 cm diameter polystyrene Petri dish). The dishes or plates were covered with two layers of Parafilm® and incubated at 37 ˚C for 21- 28 days without disturbance [27].

Plasmid constructions

The pET-15b vector (Novagen) was modified with a cleavage site for Rhinovirus protease 3C introduced between *NdeI* and *NcoI* in place of the thrombin cleavage site, leaving a sequence encoding a 5×His-tag [35].

The coding sequences corresponding to the *M. tuberculosis* H37Rv *groEL*1*, groEL*2 *and groES* genes were amplified by polymerase chain reaction (PCR). The primers used are shown in supplementary data (**Table S1**). The plasmids *p*MtGroEL1 and *p*MtGroEL1ΔHis were obtained by cloning the PCR products into the modified pET-15b vector, using the restriction sites *Nde*I and *Xho*I. The designed *p*MtGroEL1ΔHis is devoid of the last 30 bases, including the stop codon and 27 bases encoding the last 9 C-terminal amino acid residues, compared with *p*MtGroEL1. Prior to cloning, the modified pET-15b vector was linearized using the restriction enzymes *NdeI* and *BamHI*. The *M. tuberculosis groEL*2 gene was cloned into the modified pET-15b vector using

the In-Fusion® HD Cloning Kit (Clontech). The *M. tuberculosis groES* gene was cloned into the modified pET-15b vector dephosphorylated by antarctic phosphatase (Anp), using the *NdeI* restriction site. The plasmids were named *p*MtGroEL2 and *p*MtGroES, respectively. All the plasmid constructions were verified by sequencing.

Protein production and purification

The constructed plasmids were transformed into *E. coli* strain BL21(DE3) for protein production. The bacteria were grown in LB medium containing 100 μg/mL ampicillin at 37 °C. Gene expression was induced with 1 mM IPTG when the optical density reached 0.5 at 600 nm. Then, the incubation was continued for 20 hours at 18 ˚C (or 30 ˚C for GroEL2). The cells were then harvested by centrifugation at 5,000 × g and resuspended in 20 mL of 20 mM HEPES, 300 mM NaCl, 20 mM $MgSO_4$, 10 mM imidazole, pH 8.0, EDTA-free protease inhibitor cocktail (Carl Roth) and 10 μg/mL DNase (Sigma).

Protein purification was always performed at 4 ˚C [36]. The resuspended cells were homogenized in a Potter-Elvehjem homogenizer and lysed by four passages through an Emulsiflex-C3 (Avestin). The lysate was collected by centrifugation at 10,000 g and loaded onto a previously equilibrated Poly-Prep column (Bio-Rad) containing 2 mL of Ni-NTA resin (Thermo Scientific). The suspension was incubated for 1 h under gentle agitation. After collecting the column flow-through, the resin was washed with 10 mM and 40 mM imidazole, in 20 mM HEPES (pH 8.0), 300 mM NaCl. The proteins were eluted with 250 mM imidazole, 20 mM HEPES (pH 8.0), 300 mM NaCl. Prior to 5 × His-tag cleavage, the buffer was exchanged for 20 mM HEPES, 150 mM NaCl (pH 7.5) on a PD-10 desalting column (GE Healthcare). Then the protein was incubated overnight at 4 ˚C with protease 3C (protein/enzyme mass ratio of 75:1) for His-tag removal. The protein was further purified on size exclusion chromatography (SEC) using a Superdex 200 10/300 GL analytical column connected to an ÄKTA purifier system (GE Healthcare). The protein solution was eluted with a selected buffer or solution (A: 50 mM Tris-HCl, 150 mM NaCl, pH 7.5 or B: 10 mM ammonium acetate, pH 6.9).

The purified proteins were flash-frozen in liquid nitrogen and stored at -80 ˚C. Protein concentrations were determined using the calculated extinction

coefficients [37] at 280 nm: 16,960 $M^{-1}cm^{-1}$ for GroEL1 and GroEL1ΔHis, 11,460 $M^{-1}cm^{-1}$ for GroES and 15,930 $M^{-1}cm^{-1}$ for GroEL2. The purity and the integrity of recombinant proteins were determined by SDS-PAGE and denaturing mass spectrometry, respectively.

Mass spectrometry

Borosilicate nano-electrospray capillaries (Thermo Scientific) were prepared in-house using a P-97 micropipette puller (Sutter Instrument Co.) and coated with gold/palladium in a Polaron SC7620 sputter coater (Quorum Technologies). Mass spectrometers were operated in positive ion mode.

For intact mass determination, proteins were solubilized in a 50 % acetonitrile/1% formic acid (v/v) mixture after being desalted on ZipTipC4 (Millipore). Mass spectra were acquired on a Q-TOF Ultima mass spectrometer, typically using a capillary voltage of 1.8-2.0 kV and cone voltage of 50 V. The TOF analyzer was operated in the V mode. Molecular masses were determined after MaxEnt1 deconvolution of the raw m/z data (Waters).

For initial metal ion-binding studies, the protein was buffer exchanged into 10 mM ammonium acetate pH 6.9 via size exclusion chromatography. Native mass spectra were acquired on a Q-TOF Ultima mass spectrometer (Waters) using the settings described above. The metal binding specificity of proteins was determined, and each protein and metal ion were mixed at a final concentration of 10 μM. Metal ion solutions were prepared using $CoCl_2$, $ZnCl_2$, $NiCl_2$ and $CuCl_2$ salts.

Copper-binding was studied more in depth using an Orbitrap Q Exactive Plus UHMR modified for high mass range (Thermo Scientific). The protein was buffer-exchanged via SEC as described above or using two consecutive Zeba spin desalting columns (Thermo Scientific) and used at a final concentration of 7.5 μM in 500 mM ammonium acetate pH 6.9. This was found to produce less unfolded protein and allowed copper binding. Typical instrument settings were - 1.7 kV capillary voltage, - 50 V in source trapping, HCD was off and the AGC target set to 106 with a maximum inject time of 500 ms. The mass range was 2000 – 20000 m/z to allow detection of high oligomeric species if present. Raw data were analysed and processed using UniDec [38]. $CuCl_2$ was added to the sample to make final concentrations between 1.9 and 30 μM. Similar conditions

were used to study the binding of Cd^{2+} to GroEL1.

The effect of copper ion on protein thermal stability

The thermal shift assay in the presence of the fluorescent SYPRO orange dye (Invitrogen) was used to monitor protein stability [39]. The assay was conducted in 96-well plates using the CFX96TM real-time PCR system (Bio-Rad). Briefly, 25 μL of reaction mixture contained 5 μM protein (GroEL1 or GroEL1ΔHis), 0.3 μL of 5000 × SYPRO Orange, with 10 μM Cu^{2+} in 5 mM HEPES, pH 7.5. The thermocycle parameters were set up as follows: 20 minutes pause at 10 ˚C, followed by a melt curve recorded from 10 ˚C to 95 ˚C, with 1 ˚C increase every minute, then pause at 10 ˚C for 10 minutes. The fluorescence intensity was recorded at Ex/Em = 465/510 nm. The data were obtained from the Bio-Rad Precision Melt Analysis software 1.0 and exported as Microsoft Excel spreadsheet.

Trypsin digestion susceptibility assay

To investigate the effect of copper ions on protease digestion susceptibility, a trypsin digestion assay was performed as previously described with minor modifications [40] on GroEL1 or GroEL1ΔHis in the presence or absence of Cu^{2+} at 37 ˚C. Briefly, the reaction mixture contained 5 μg GroEL1 or GroEL1ΔHis, 0.0015 μg trypsin (a mass ration of protein to trypsin was 10,000:3), in the presence or absence of $CuCl_2$. The reaction was terminated at various times by adding 1.5 μL of 50 mM PMSF and 7.5 μL SDS-PAGE Laemmli buffer (2×) to 6 μL aliquots of the reaction mixture, and the resulting solution was immediately frozen in liquid nitrogen. The samples were finally analysed by SDS-PAGE on a 15 % polyacrylamide gel. In addition, the influence of copper on trypsin activity was evaluated using *Nα*-benzoyl-DL-arginine 4-nitroanilide hydrochloride (BAPNA, Sigma) as substrate [41].

ATPase activity assay

The ATPase activities of the purified recombinant mycobacteria GroEL (GroEL1, GroEL1ΔHis, GroEL2) were quantified using a slightly modified colorimetric assay [42]. Briefly, 100 μL of the reaction buffer containing 10 mM KCl, 2 mM ATP, 10 mM $MgCl_2$, 50 mM Tris-HCl (pH 7.5), 150 mM NaCl, and 10 μM proteins, in the absence or the presence of 20 μM GroES were incubated for 1 hour at 37 ˚C. Enzymatic reactions were terminated by addition of 500 μL

of 1% SDS. Colour development was measured as follows: 200 μL of ammonium molybdate reagent was added to each tube immediately followed by the addition of 200 μl Elon reagent. After 15 min at room temperature, the absorbance of the final solution (200 μL of reactions in 96 well-plates) was measured at 700 nm. Control experiments without protein were always included. The recombinant *E. coli* GroEL was from Abcam.

To investigate the effect of metal ions on ATPase activity, the same experiment was performed in the presence of 100 μM of metal ions (Ni^{2+}, Cu^{2+}, Cd^{2+}, Zn^{2+} or Co^{2+}).

Structural modelling of GroEL1

A BLAST search performed on the Protein Data Bank (PDB) sequences identified GroEL2 from *M. tuberculosis* as a potential template for building a GroEL1 model. Two 3D models of GroEL1 were built by comparative modelling with Modeller 9v11 [43] using the *M. tuberculosis* Cpn60.2 (GroEL2) crystal structure as a template [44] and the sequence alignment carried out with ClustalW. The ATP analogue was positioned based on the superposed GroEL structure (PDB ID: 1SX3) [45] to predict the potential ATP binding site.

Results and discussion

GroEL1 increase copper tolerance during *M. bovis* BCG biofilm formation

The impact of metal ions was evaluated on the biofilm growth of *M. bovis* BCG strains. As the Δ*groEL1* BCG (KO) strain is more sensitive to glycerol osmotic stress [11], the amount of glycerol in the biofilm culture was reduced to 3.5% (instead of the usual 6%) in order to allow biofilm production by the Δ*groEL1* BCG (KO) strain. The wild type (wt) BCG strain was able to form mature biofilm (with ridges and troughs) in the presence of Cu^{2+} concentrations up to 175 μM, but from 200 μM Cu^{2+} the biofilm growth was inhibited (**Figure 1**). The Δ*groEL*1 BCG (KO) strain showed a higher susceptibility to copper, losing the ability to form mature biofilm at 125 μM Cu^{2+}, leading to absence of biofilm in the presence of 150 μM Cu^{2+}. The *groEL*1 gene complementation in the KO strain (compl. BCG) restored biofilm growth with similar phenotype as the wt BCG strain (**Figure 1**). This protective effect of GroEL1 was only observed in biofilm culture and not in the planktonic culture. Indeed, the minimum inhibitory concentration (MIC) for $CuCl_2$ was identical for the three strains in rich medium, such as the 7H9 medium (data not shown). This suggests that under stressful environments, *M. bovis* GroEL1 increases tolerance to high toxic copper concentrations. Therefore, GroEL1 could potentially protect mycobacteria from the bactericidal copper excess present in the macrophage phagosome [32]. Indeed, copper is both essential and toxic for *M. tuberculosis*. Although copper is a critical cofactor for various mycobacterial enzymes, notably essential for enzymes to resist oxidative stress, *i.e.* electron transfer reactions, cytochrome *c* oxidase and Cu/Cu superoxide dismutase, high copper concentrations are bactericidal [46, 47].

Biofilm growth was also evaluated in the presence of increasing concentrations of Zn^{2+} and Cd^{2+}. As shown in **Figure S1**, no significant difference in biofilm growth susceptibility was observed among the three *M. bovis* BCG strains. Biofilm cultures were unaffected by Zn^{2+} at concentrations up to 600 μM, which is even above the Zn^{2+} concentration inside the infected macrophages [31]. Cadmium ions similarly affected biofilm growth at 5 μM for the three strains.

Taken together, these observations indicate that high concentrations of

Cu^{2+} could reduce *M. bovis* BCG biofilm maturation, and that GroEL1 is required to resist to toxic Cu^{2+} concentration under this stress condition. Recently, Ansari *et al*. observed similar results using *M. tuberculosis* strains, however in normal growth condition [34]. They didn't investigate the role of GroEL1 under stress conditions [34]. The fact that they observed an involvement of GroEL1 in planktonic growth conditions, while this was not detected by our group, could be due either to the use of a different mycobacterium species or to our optimal planktonic growth conditions for *M. bovis* BCG (*i.e.* optimized albumin quality), leading to less GroEL1 production in our planktonic cultures.

Usually, copper resistance mechanisms involve copper specific chaperones, storage proteins and efflux systems [48]. CtpV, a predicted P-type ATPase, has been shown to be a copper efflux pump in the mycobacterial plasma membrane and is required for resistance to copper toxicity [49]. MctB, mycobacterial copper transport protein B, essential for maintaining low Cu concentration in mycobacteria, could be a putative copper transport protein at the outer membrane [50]. The metallothionein MymT, a cysteine-rich protein, able to bind up to six Cu^{+}, is also partially involved in copper toxicity resistance, suggesting that it could play the role of a storage protein [51]. Furthermore, a copper inducible *M. tuberculosis* operon, including *lpqS* (encoding a putative lipoprotein), *mmcO* (encoding a mycobacterial multicopper oxidase), *Rv2963* (encoding a possible permease), *mymT* (encoding the metallothionein described above), *socAB* (small ORF induced by Cu A and B) and *ricR* (encoding a repressor of this operon) genes, seems to provide key components of an additional system involved in copper detoxification [30]. The different pathways previously reported [30, 52] could help to keep the copper homeostasis in *M. tuberculosis*. However, all these systems seem to lack a key component: a copper chaperone which could transfer copper to the various copper binding proteins and efflux pumps [30]. As GroEL1 can be secreted in the culture filtrate, further investigation about copper affinity for GroEL1 was performed.

The native histidine-rich region affects GroEL1 stability

To study the role of the C-terminal histidine-rich region (HDHHHGHAH) of GroEL1, the recombinant *M. bovis* BCG proteins GroEL1 and a *M. bovis* GroEL1 devoid of the C-terminal histidine-rich region (GroEL1ΔHis) were

purified. These proteins were overproduced in the *E. coli* BL21(DE3) strain, purified by immobilized metal affinity chromatography, treated with human rhinovirus 3C protease for the additional 5×His-tag cleavage, and then further purified by size exclusion chromatography (SEC). The purity and the integrity of recombinant proteins were analysed by SDS-PAGE and mass spectrometry, respectively (**Figure S2**). Mass spectrometry data clearly indicated that the additional N-terminal 5×His-tag was removed in both proteins.

Recombinant GroEL1 was eluted in SEC as a single peak but migrated as two bands in SDS-PAGE analysis, i.e. an upper stronger band followed by a weaker band **(Figure S2 A)**. Peptide sequence analysis by mass spectrometry demonstrated that the weak band corresponds to a degradation product of GroEL1 lacking the N-terminal region (about 45 amino acid residues missing out of 543) (data not shown). This proteolysis was not observed for the GroEL1ΔHis, always showing a single band in SDS-PAGE analysis **(Figure S2 B)**.

Although various conditions were tested, for instance, pH modification and glycerol addition, the GroEL1 purification efficiency always lead to N-terminal proteolysis. As GroEL1ΔHis appeared to be less prone to proteolysis than GroEL1 under the present purification conditions, these results suggest that GroEL1 histidine-rich region affects the protein stability.

GroEL1-copper interaction analysed by native mass spectrometry

Brazil *et al*. reported that the divalent cations (Ca^{2+}, Mg^{2+}, Mn^{2+}, Zn^{2+}) induce exposure of the *E. coli* GroEL hydrophobic surfaces and strengthen the GroEL hydrophobic binding interactions [53]. This was attributed to a conformation change of GroEL when binding to the divalent cations [54]. To further investigate the interaction between GroEL1 and Cu^{2+}, the metal binding specificity of *M. tuberculosis* GroEL proteins was monitored by native mass spectrometry. Native mass spectra were recorded after incubation of the proteins with or without Cu^{2+}. Importantly, the addition of one molar equivalent of Cu^{2+} induced a shift of the GroEL1 peak to a higher m/z value corresponding to the binding of one atom of copper to the protein (**Figure 2A**). The nearly complete disappearance of the apo peak upon copper addition reflects an effective binding of this metal ion to GroEL1. In contrast, practically no

conversion of the apo to the holo form was observed upon addition of one molar equivalent of Cu^{2+} to GroEL1ΔHis (**Figure 2B**). This observation suggests that the Cu^{2+} is mainly bound to the histidine-rich region of GroEL1.

Moreover, the ability of other metal ions (*i.e.* Zn^{2+}, Ni^{2+}, Cd^{2+} and Co^{2+}) to bind to GroEL1 was also assessed (**Figure S3 and S4**). The binding of Zn^{2+} and Ni^{2+} to GroEL1 was also observed but with a lower efficiency than for Cu^{2+} (**Figure S3**). At a metal/protein ratio of 1:1, there were nearly no binding of Cd^{2+} to GroEL1. To further study the copper binding to the protein, GroEL1 was titrated with increasing amounts of Cu^{2+} and analysed by native mass spectrometry (**Figure 3**). Sequential addition of Cu^{2+} led to the appearance of the holo form GroEL1·Cu which was the main population observed at the GroEL1/Cu^{2+} 1:1 molar ratio, as described in the previous experiment. At higher molar ratios, GroEL1·2Cu and GroEL1·3Cu populations were detected with a concomitant decrease of the GroEL1·Cu abundance. On the contrary, in the same range of Cu^{2+} concentrations, the apo form of GroEL1ΔHis did not totally disappear and the highest stoichiometry for the protein/metal complex observed in the presence of four molar equivalents of copper was GroEL1ΔHis·2Cu. These results suggest that GroEL1 preferentially binds copper ions and that the protein possesses different binding sites with most probably different affinities for the copper ions. The presence of binding sites with different affinities for copper ions was also observed for GroEL1 by isothermal titration calorimetry (ITC) analysis [34]. For the sake of comparison, the recombinant GroEL2 was also purified (**Figure S2**), and the binding of copper to GroEL2 was also investigated. The binding of copper to GroEL2 gave similar results that the GroEL1ΔHis (**Figure 3**).

The effect of copper on *M. tuberculosis* GroEL1 protein oligomeric state was also investigated by native mass spectrometry (**Figure S5**). The recombinant GroEL1 is mainly monomeric with small amounts of dimeric protein, in agreement with a previous report [55]. The same observations were obtained for the GroEL1ΔHis and GroEL2 (data not shown). Moreover, when adding Cu^{2+}, the overall spectra for GroEL1 and GroEL1ΔHis did not change significantly in the range of 0 to 30 μM $CuCl_2$, indicating that higher oligomers could not be observed under these conditions.

The effect of copper on GroEL1 thermal stability

Thermal shift assays were performed to evaluate the effect of Cu^{2+} on protein stability. The use of the SYPRO orange fluorescent dye and a real-time thermocycler to follow thermal denaturation in different conditions enabled the monitoring of GroEL1 and GroEL1ΔHis stability in the presence of Cu^{2+}. It was showed that the Tm values for GroEL1 were higher than for GroEL1ΔHis in the presence of Cu^{2+} (10 to 50 μM) (**Figure 4**). Although high Cu^{2+} concentrations are deleterious for both proteins, the difference in Tm values suggests that the binding of copper to the histidine-rich region could have a protective effect as the binding of the metal ions is more efficient on GroEL1 than on GroEL1ΔHis.

Protease susceptibility assay

To further investigate whether Cu^{2+} could increase the GroEL1 protein stability, a mild trypsin digestion was performed in the absence or the presence of Cu^{2+}. The GroEL1 displayed a higher tolerance to trypsin digestion in the presence of Cu^{2+} (**Figure 5**). In addition, the degree of tolerance increased with the copper concentration (**Figure S6**). The binding of Cu^{2+} to the GroEL1 protein improves thus its stability. A similar result was also observed with GroEL1ΔHis (**Figure 5**). A control was performed using *Nα*-benzoyl-DL-arginine 4-nitroanilide hydrochloride (BAPNA) as substrate and demonstrated that the trypsin activity was not affected by the presence of Cu^{2+} and that the protease even displayed a small increase of activity in the range of copper concentrations used in the experiment (data not shown), as previously reported [56]. The fact that the trypsin susceptibility was also decreased for GroEL1ΔHis in the presence of Cu^{2+}, suggests that conformational changes could also occur in the protein upon Cu^{2+} binding to the other coordination sites.

Copper increases the GroEL1 ATPase activity

ATP hydrolysis by the recombinant *M. tuberculosis* GroEL proteins was investigated in the presence or absence of metal ions. *M. tuberculosis* GroEL1 and GroEL2 displayed weak ATPase activity, with a higher activity for GroEL2 than for GroEL1 (**Figure 6**). Surprisingly, the GroEL1ΔHis showed a two-fold increased ATPase activity compared to GroEL1. GroEL1ΔHis and GroEL2 had almost the same activity (**Figure 6**). The presence of GroES, also produced and purified for this study (**Figure S2**), had no impact on GroEL1 and GroEL2

in vitro ATPase activities, in agreement with previous studies [55, 57]. The GroEL1 ATPase activity was increased about eight-fold in the presence of Cu^{2+} (**Figure 7**). This effect was not observed for GroEL1ΔHis and GroEL2. The other metal ions tested (Ni^{2+}, Co^{2+}, Cd^{2+} or Zn^{2+}) did not influence the GroEL1 protein activity, although the presence of Co^{2+} slightly increased the GroEL1ΔHis and the GroEL2 ATPase activities. The effect of Cu^{2+} and Co^{2+} on recombinant *E. coli* GroEL ATPase activity was also evaluated and showed that these metal ions had no effect on its ATPase activity (**Figure S7**).

GroEL1 three-dimensional model

To better understand the impact of the histidine-rich C-terminal region on the N-terminal region stability, a GroEL1 three-dimensional structure model was built using the crystal structure of *M. tuberculosis* GroEL2 (PDB ID: 3RTK) [44] as template. Both proteins share 62% sequence identity (86% sequence similarity) in 527 residues overlap. It is worth noting that in the crystal structure of GroEL2, the conformation of the 60 first N-terminal residues and of the 26 last C-terminal residues was not solved, most probably due to the flexibility of these domains. The C-terminal residues are also absent in the published structures of the *E. coli* GroEL (*e.g.* PDB ID: 1GRL, 1OEL) [58, 59]. The model of GroEL1 in the present study suggests that the N- and C-terminal domains of the protein could be close to each other in the equatorial domain of the protein (**Figure 8**). As the recombinant GroEL1ΔHis is less prone to the N-terminal proteolytic degradation during purification (**Figure S2**), we hypothesize that the histidine-rich region in GroEL1 somehow increases the accessibility of the latter to proteolytic enzymes

Interestingly, Ansari *et al*., built a GroEL1 3D model based on their small angle X-ray scattering (SAXS) data obtained in the presence of various GroEL1/Cu^{2+} ratios [34]. The SAXS analysis suggested that the protein adopts a more open structure in the presence of Cu^{2+}, and becomes more flexible. These conformational changes could be responsible for the increase of GroEL1 ATPase activity observed in our study in the presence of copper ions. As the protein is predicted to be more extended and flexible in the presence of Cu^{2+}, it would be expected that GroEL1 would be more susceptible to protease activity. However, this is not what was observed as our limited trypsin digestion assay

461 suggesting that the protein, especially the N-terminal region, is less accessible
462 to the protease in the presence of Cu^{2+}.
463

Conclusions

Mycobacterial GroEL1 plays important roles in *M. tuberculosis* adaptation to the environment, such as resistance to antibiotic and other various stressful conditions [11, 22, 60]. In this context, the results indicated that under stressful environments *M. bovis* BCG GroEL1 increases tolerance to high toxic copper concentrations. Using native mass spectrometry, we demonstrated the specific binding of copper ions to GroEL1, having a higher affinity for the histidine-rich C-terminal domain. Up to two other binding sites with a lower affinity are most probably present in the protein as deduced from the comparison of the copper binding profiles of GroEL1 and GroEL1ΔHis. The presence of these binding sites strongly suggests that GoEL1 could segregate *in vivo* the copper ions present in the macrophages and therefore, by decreasing the concentration of free ions, protect the bacteria from the toxic effect of these metal ions.

Apart from this protective role against higher bactericidal copper concentration, the binding of copper ions to GroEL1 could have also an additional function to improve the GroEL1 N-terminal region stability. Based on our GroEL1 3D model, it is possible that the N- and C-terminal domains of the protein could be close to each other and that the binding of copper ions to the histidine-rich domain could affect the interaction of C-terminal segment with the N-terminal domain thereby reducing the exposure of the latter to proteases. Nevertheless, copper binding is not inducing a modification of the GroEL1 oligomeric state, as demonstrated by native mass spectrometry analysis.

Importantly, the GroEL1 ATPase activity is drastically and specifically increased in the presence of Cu^{2+}, mainly binding to the histidine-rich region. This is only observed for GroEL1 and not for GroEL1ΔHis, GroEL2 and GroEL from *E. coli,* suggesting that the binding of copper ions to the GroEL1 histidine-rich C-terminal region induces a conformational change allowing to increase its ATPase activity. For GroEL1ΔHis and GroEL2, both lacking the histidine-rich region, it is possible that they displayed higher ATPase activity than the GroEL1 because of higher protein stability.

Here, we propose a novel role for the *M. tuberculosis* GroEL1. This protein could be involved in copper resistance during mycobacterial biofilm formation potentially by acting as a metal storage protein. Therefore, when mycobacteria

encounter high copper concentrations, as in the macrophage, GroEL1, by binding copper, could help bacteria to tolerate high copper concentrations and consequently this bactericidal stress [5, 11].

Conflicts of interest

The authors declare that they have no conflicts of interest with the content of this article.

Acknowledgment

This work was partially supported by the China Scholarship Council (CSC) (No.201408210159). F.S. and D.P.K. would like to thank James Ault and Rachel George for their help operating the Orbitrap UHMR. The Orbitrap UHMR was funded by Wellcome Trust multi-user equipment grant 208385/Z/17/Z.

References

1. WHO, Global tuberculosis report, *World Health Organization*, 2019.
2. P. J. Brennan and H. Nikaido, The envelope of mycobacteria, *Annu Rev Biochem*, 1995, **64**, 29-63.
3. M. Jankute, J. A. Cox, J. Harrison and G. S. Besra, Assembly of the Mycobacterial Cell Wall, *Annu Rev Microbiol*, 2015, **69**, 405-423.
4. L. R. Camacho, P. Constant, C. Raynaud, M. A. Laneelle, J. A. Triccas, B. Gicquel, M. Daffe and C. Guilhot, Analysis of the phthiocerol dimycocerosate locus of *Mycobacterium tuberculosis*. Evidence that this lipid is involved in the cell wall permeability barrier, *The Journal of biological chemistry*, 2001, **276**, 19845-19854.
5. K. Soetaert, C. Rens, X. M. Wang, J. De Bruyn, M. A. Laneelle, F. Laval, A. Lemassu, M. Daffe, P. Bifani, V. Fontaine and P. Lefevre, Increased Vancomycin Susceptibility in Mycobacteria: a New Approach To Identify Synergistic Activity against Multidrug-Resistant Mycobacteria, *Antimicrobial agents and chemotherapy*, 2015, **59**, 5057-5060.
6. C. W. Hall and T. F. Mah, Molecular mechanisms of biofilm-based antibiotic resistance and tolerance in pathogenic bacteria, *FEMS Microbiol Rev*, 2017, **41**, 276-301.
7. A. Queiroz and L. W. Riley, Bacterial immunostat: *Mycobacterium tuberculosis* lipids and their role in the host immune response, *Rev Soc Bras Med Trop*, 2017, **50**, 9-18.
8. V. Sundaramurthy, H. Korf, A. Singla, N. Scherr, L. Nguyen, G. Ferrari, R. Landmann, K. Huygen and J. Pieters, Survival of *Mycobacterium tuberculosis* and *Mycobacterium bovis* BCG in lysosomes in vivo, *Microbes Infect*, 2017, **19**, 515-526.
9. A. M. Alnimr, Dormancy models for *Mycobacterium tuberculosis*: A minireview, *Braz J Microbiol*, 2015, **46**, 641-647.

10. R. D. Turner, C. Chiu, G. J. Churchyard, H. Esmail, D. M. Lewinsohn, N. R. Gandhi and K. P. Fennelly, Tuberculosis Infectiousness and Host Susceptibility, *J Infect Dis*, 2017, **216**, S636-S643.
11. S. Zeng, P. Constant, D. Yang, A. Baulard, P. Lefevre, M. Daffe, R. Wattiez and V. Fontaine, Cpn60.1 (GroEL1) Contributes to Mycobacterial Crabtree Effect: Implications for Biofilm Formation, *Front Microbiol*, 2019, **10**, 1149.
12. T. H. Kong, A. R. Coates, P. D. Butcher, C. J. Hickman and T. M. Shinnick, *Mycobacterium tuberculosis* expresses two chaperonin-60 homologs, *Proceedings of the National Academy of Sciences of the United States of America*, 1993, **90**, 2608-2612.
13. A. Ojha, M. Anand, A. Bhatt, L. Kremer, W. R. Jacobs and G. F. Hatfull, GroEL1: A Dedicated Chaperone Involved in Mycolic Acid Biosynthesis during Biofilm Formation in Mycobacteria, *Cell*, 2005, **123**, 861-873.
14. C. Chaudhry, G. W. Farr, M. J. Todd, H. S. Rye, A. T. Brunger, P. D. Adams, A. L. Horwich and P. B. Sigler, Role of the gamma-phosphate of ATP in triggering protein folding by GroEL-GroES: function, structure and energetics, *EMBO J*, 2003, **22**, 4877-4887.
15. H. S. Rye, A. M. Roseman, S. Chen, K. Furtak, W. A. Fenton, H. R. Saibil and A. L. Horwich, GroEL-GroES cycling: ATP and nonnative polypeptide direct alternation of folding-active rings, *Cell*, 1999, **97**, 325-338.
16. T. E. Gray and A. R. Fersht, Cooperativity in ATP hydrolysis by GroEL is increased by GroES, *FEBS Lett*, 1991, **292**, 254-258.
17. M. J. Todd, P. V. Viitanen and G. H. Lorimer, Hydrolysis of adenosine 5'-triphosphate by *Escherichia coli* GroEL: effects of GroES and potassium ion, *Biochemistry*, 1993, **32**, 8560-8567.
18. P. V. Viitanen, T. H. Lubben, J. Reed, P. Goloubinoff, D. P. O'Keefe and G. H. Lorimer, Chaperonin-facilitated refolding of ribulose bisphosphate carboxylase and ATP hydrolysis by chaperonin 60 (groEL) are K^+

dependent, *Biochemistry*, 1990, **29**, 5665-5671.

19. G. C. Melkani, G. Zardeneta and J. A. Mendoza, The ATPase activity of GroEL is supported at high temperatures by divalent cations that stabilize its structure, *Biometals : an international journal on the role of metal ions in biology, biochemistry, and medicine*, 2003, **16**, 479-484.
20. G. R. Stewart, L. Wernisch, R. Stabler, J. A. Mangan, J. Hinds, K. G. Laing, D. B. Young and P. D. Butcher, Dissection of the heat-shock response in *Mycobacterium tuberculosis* using mutants and microarrays, *Microbiology*, 2002, **148**, 3129-3138.
21. N. S. Dosanjh, M. Rawat, J. H. Chung and Y. Av-Gay, Thiol specific oxidative stress response in Mycobacteria, *FEMS Microbiol Lett*, 2005, **249**, 87-94.
22. X. M. Wang, C. Lu, K. Soetaert, C. S'Heeren, P. Peirs, M. A. Laneelle, P. Lefevre, P. Bifani, J. Content, M. Daffe, K. Huygen, J. De Bruyn and R. Wattiez, Biochemical and immunological characterization of a *cpn60.1* knockout mutant of *Mycobacterium bovis* BCG, *Microbiology*, 2011, **157**, 1205-1219.
23. Y. Hu, B. Henderson, P. A. Lund, P. Tormay, M. T. Ahmed, S. S. Gurcha, G. S. Besra and A. R. Coates, A *Mycobacterium tuberculosis* mutant lacking the *groEL* homologue *cpn60.1* is viable but fails to induce an inflammatory response in animal models of infection, *Infect Immun*, 2008, **76**, 1535-1546.
24. I. M. Monahan, J. Betts, D. K. Banerjee and P. D. Butcher, Differential expression of mycobacterial proteins following phagocytosis by macrophages, *Microbiology*, 2001, **147**, 459-471.
25. J. Esteban and M. Garcia-Coca, Mycobacterium Biofilms, *Front Microbiol*, 2017, **8**, 2651.
26. G. Carter, M. Wu, D. C. Drummond and L. E. Bermudez, Characterization

595 of biofilm formation by clinical isolates of *Mycobacterium avium*, *J Med*
596 *Microbiol*, 2003, **52**, 747-752.
597 27. A. K. Ojha, A. D. Baughn, D. Sambandan, T. Hsu, X. Trivelli, Y. Guerardel,
598 A. Alahari, L. Kremer, W. R. Jacobs, Jr. and G. F. Hatfull, Growth of
599 *Mycobacterium tuberculosis* biofilms containing free mycolic acids and
600 harbouring drug-tolerant bacteria, *Molecular microbiology*, 2008, **69**, 164-
601 174.
602 28. H. Botella, P. Peyron, F. Levillain, R. Poincloux, Y. Poquet, I. Brandli, C.
603 Wang, L. Tailleux, S. Tilleul, G. M. Charriere, S. J. Waddell, M. Foti, G.
604 Lugo-Villarino, Q. Gao, I. Maridonneau-Parini, P. D. Butcher, P. R.
605 Castagnoli, B. Gicquel, C. de Chastellier and O. Neyrolles, Mycobacterial
606 p(1)-type ATPases mediate resistance to zinc poisoning in human
607 macrophages, *Cell Host Microbe*, 2011, **10**, 248-259.
608 29. V. Hodgkinson and M. J. Petris, Copper homeostasis at the host-pathogen
609 interface, *The Journal of biological chemistry*, 2012, **287**, 13549-13555.
610 30. X. Shi and K. H. Darwin, Copper homeostasis in *Mycobacterium*
611 *tuberculosis*, *Metallomics : integrated biometal science*, 2015, **7**, 929-934.
612 31. D. Wagner, J. Maser, B. Lai, Z. Cai, C. E. Barry, K. Honer zu Bentrup, D.
613 G. Russell and L. E. Bermudez, Elemental Analysis of *Mycobacterium*
614 *avium*-, *Mycobacterium tuberculosis*-, and *Mycobacterium smegmatis*-
615 Containing Phagosomes Indicates Pathogen-Induced Microenvironments
616 within the Host Cell's Endosomal System, *The Journal of Immunology*,
617 2005, **174**, 1491-1500.
618 32. F. Wolschendorf, D. Ackart, T. B. Shrestha, L. Hascall-Dove, S. Nolan, G.
619 Lamichhane, Y. Wang, S. H. Bossmann, R. J. Basaraba and M. Niederweis,
620 Copper resistance is essential for virulence of *Mycobacterium tuberculosis*,
621 *Proceedings of the National Academy of Sciences of the United States of*
622 *America*, 2011, **108**, 1621-1626.

623 33. O. Neyrolles, F. Wolschendorf, A. Mitra and M. Niederweis, Mycobacteria,
624 metals, and the macrophage, *Immunological reviews*, 2015, **264**, 249-263.
625 34. M. Y. Ansari, S. D. Batra, H. Ojha, Ashish, J. S. Tyagi and S. C. Mande, A
626 novel function of *M. tuberculosis* chaperonin paralog GroEL1 in copper
627 homeostasis, *bioRxiv*, 2019, DOI: 10.1101/766162, 766162.
628 35. D. Yang, G. Vandenbussche, D. Vertommen, D. Evrard, R. Abskharon, J.
629 F. Cavalier, G. Berger, S. Canaan, M. S. Khan, S. Zeng, A. Wohlkonig, M.
630 Prevost, P. Soumillion and V. Fontaine, Methyl arachidonyl
631 fluorophosphonate inhibits *Mycobacterium tuberculosis* thioesterase TesA
632 and globally affects vancomycin susceptibility, *FEBS Lett*, 2020, **594**, 79-
633 93.
634 36. C. Structural Genomics, C. China Structural Genomics, C. Northeast
635 Structural Genomics, S. Graslund, P. Nordlund, J. Weigelt, B. M. Hallberg,
636 J. Bray, O. Gileadi, S. Knapp, U. Oppermann, C. Arrowsmith, R. Hui, J.
637 Ming, S. dhe-Paganon, H. W. Park, A. Savchenko, A. Yee, A. Edwards, R.
638 Vincentelli, C. Cambillau, R. Kim, S. H. Kim, Z. Rao, Y. Shi, T. C. Terwilliger,
639 C. Y. Kim, L. W. Hung, G. S. Waldo, Y. Peleg, S. Albeck, T. Unger, O. Dym,
640 J. Prilusky, J. L. Sussman, R. C. Stevens, S. A. Lesley, I. A. Wilson, A.
641 Joachimiak, F. Collart, I. Dementieva, M. I. Donnelly, W. H. Eschenfeldt, Y.
642 Kim, L. Stols, R. Wu, M. Zhou, S. K. Burley, J. S. Emtage, J. M. Sauder, D.
643 Thompson, K. Bain, J. Luz, T. Gheyi, F. Zhang, S. Atwell, S. C. Almo, J. B.
644 Bonanno, A. Fiser, S. Swaminathan, F. W. Studier, M. R. Chance, A. Sali,
645 T. B. Acton, R. Xiao, L. Zhao, L. C. Ma, J. F. Hunt, L. Tong, K. Cunningham,
646 M. Inouye, S. Anderson, H. Janjua, R. Shastry, C. K. Ho, D. Wang, H.
647 Wang, M. Jiang, G. T. Montelione, D. I. Stuart, R. J. Owens, S. Daenke, A.
648 Schutz, U. Heinemann, S. Yokoyama, K. Bussow and K. C. Gunsalus,
649 Protein production and purification, *Nat Methods*, 2008, **5**, 135-146.
650 37. M. R. Wilkins, E. Gasteiger, A. Bairoch, J. C. Sanchez, K. L. Williams, R.

D. Appel and D. F. Hochstrasser, Protein identification and analysis tools in the ExPASy server, *Methods Mol Biol*, 1999, **112**, 531-552.

38. M. T. Marty, A. J. Baldwin, E. G. Marklund, G. K. Hochberg, J. L. Benesch and C. V. Robinson, Bayesian deconvolution of mass and ion mobility spectra: from binary interactions to polydisperse ensembles, *Anal Chem*, 2015, **87**, 4370-4376.
39. K. Huynh and C. L. Partch, Analysis of protein stability and ligand interactions by thermal shift assay, *Curr Protoc Protein Sci*, 2015, **79**, 28 29 21-28 29 14.
40. H. Kawasaki, Y. Kurosu, H. Kasai, T. Isobe and T. Okuyama, Limited digestion of calmodulin with trypsin in the presence or absence of various metal ions, *J Biochem*, 1986, **99**, 1409-1416.
41. I. Kurtovic, S. N. Marshall and B. K. Simpson, Isolation and characterization of a trypsin fraction from the pyloric ceca of chinook salmon (*Oncorhynchus tshawytscha*), *Comp Biochem Physiol B Biochem Mol Biol*, 2006, **143**, 432-440.
42. , Biomembranes. Part Q. ATP-driven pumps and related transport: calcium, proton, and potassium pumps, *Methods Enzymol*, 1988, **157**, 1-731.
43. A. Fiser and A. Sali, Modeller: generation and refinement of homology-based protein structure models, *Methods Enzymol*, 2003, **374**, 461-491.
44. A. Shahar, M. Melamed-Frank, Y. Kashi, L. Shimon and N. Adir, The dimeric structure of the Cpn60.2 chaperonin of *Mycobacterium tuberculosis* at 2.8 Å reveals possible modes of function, *J Mol Biol*, 2011, **412**, 192-203.
45. D. K. Clare, P. J. Bakkes, H. van Heerikhuizen, S. M. van der Vies and H. R. Saibil, An expanded protein folding cage in the GroEL-gp31 complex, *J Mol Biol*, 2006, **358**, 905-911.
46. L. Spagnolo, I. Toro, M. D'Orazio, P. O'Neill, J. Z. Pedersen, O. Carugo, G.

679 Rotilio, A. Battistoni and K. Djinovic-Carugo, Unique features of the *sodC*-
680 encoded superoxide dismutase from *Mycobacterium tuberculosis*, a fully
681 functional copper-containing enzyme lacking zinc in the active site, *The*
682 *Journal of biological chemistry*, 2004, **279**, 33447-33455.
683 47. S. K. Ward, B. Abomoelak, E. A. Hoye, H. Steinberg and A. M. Talaat, CtpV:
684 a putative copper exporter required for full virulence of *Mycobacterium*
685 *tuberculosis*, *Molecular microbiology*, 2010, **77**, 1096-1110.
686 48. T. D. Rae, P. J. Schmidt, R. A. Pufahl, V. C. Culotta and T. V. O'Halloran,
687 Undetectable intracellular free copper: the requirement of a copper
688 chaperone for superoxide dismutase, *Science*, 1999, **284**, 805-808.
689 49. S. K. Ward, E. A. Hoye and A. M. Talaat, The global responses of
690 *Mycobacterium tuberculosis* to physiological levels of copper, *J Bacteriol*,
691 2008, **190**, 2939-2946.
692 50. A. Senju and G. Csibra, Gaze following in human infants depends on
693 communicative signals, *Curr Biol*, 2008, **18**, 668-671.
694 51. B. Gold, H. Deng, R. Bryk, D. Vargas, D. Eliezer, J. Roberts, X. Jiang and
695 C. Nathan, Identification of a copper-binding metallothionein in pathogenic
696 mycobacteria, *Nat Chem Biol*, 2008, **4**, 609-616.
697 52. M. I. Samanovic, C. Ding, D. J. Thiele and K. H. Darwin, Copper in
698 microbial pathogenesis: meddling with the metal, *Cell Host Microbe*, 2012,
699 **11**, 106-115.
700 53. B. T. Brazil, J. Ybarra and P. M. Horowitz, Divalent cations can induce the
701 exposure of GroEL hydrophobic surfaces and strengthen GroEL
702 hydrophobic binding interactions. Novel effects of Zn^{2+} GroEL interactions,
703 *The Journal of biological chemistry*, 1998, **273**, 3257-3263.
704 54. D. L. Gibbons and P. M. Horowitz, Ligand-induced conformational changes
705 in the apical domain of the chaperonin GroEL, *The Journal of biological*
706 *chemistry*, 1996, **271**, 238-243.

55. R. Qamra, V. Srinivas and S. C. Mande, *Mycobacterium tuberculosis* GroEL homologues unusually exist as lower oligomers and retain the ability to suppress aggregation of substrate proteins, *J Mol Biol*, 2004, **342**, 605-617.
56. H. Steinhart, R. Wieninger-Rustemeyer and M. Kirchgessner, Effect of Cu^{2+} ions on the activity of trypsin on natural substance, *Arch Tierernahr*, 1981, **31**, 119-125.
57. C. M. Kumar, G. Khare, C. V. Srikanth, A. K. Tyagi, A. A. Sardesai and S. C. Mande, Facilitated oligomerization of mycobacterial GroEL: evidence for phosphorylation-mediated oligomerization, *J Bacteriol*, 2009, **191**, 6525-6538.
58. K. Braig, Z. Otwinowski, R. Hegde, D. C. Boisvert, A. Joachimiak, A. L. Horwich and P. B. Sigler, The crystal structure of the bacterial chaperonin GroEL at 2.8 Å, *Nature*, 1994, **371**, 578-586.
59. K. Braig, P. D. Adams and A. T. Brunger, Conformational variability in the refined structure of the chaperonin GroEL at 2.8 Å resolution, *Nat Struct Biol*, 1995, **2**, 1083-1094.
60. A. Sharma, T. Rustad, G. Mahajan, A. Kumar, K. V. Rao, S. Banerjee, D. R. Sherman and S. C. Mande, Towards understanding the biological function of the unusual chaperonin Cpn60.1 (GroEL1) of *Mycobacterium tuberculosis*, *Tuberculosis (Edinb)*, 2016, **97**, 137-146.

Supplementary information

Figure S1. The impact of Zn^{2+} and Cd^{2+} on the various *M. bovis* BCG strains biofilm formation.

Figure S2. Recombinant protein purity and integrity determination.

Figure S3. Native nano-ESI mass spectra of GroEL1 in the absence or presence of Zn^{2+}, Ni^{2+} or Co^{2+}.

Figure S4. Native nano-ESI mass spectra of GroEL1 in the absence or presence of Cd^{2+}.

Figure S5. GroEL1 oligomeric state determination by native mass spectrometry.

Figure S6. Protection of GroEL1 from limited trypsin digestion in a Cu^{2+} concentration dependent manner.

Figure S7. *E. coli* GroEL ATPase activity in the presence of Cu^{2+} and Co^{2+}.

Table S1. Plasmids and oligonucleotide primers.

Figure Legends

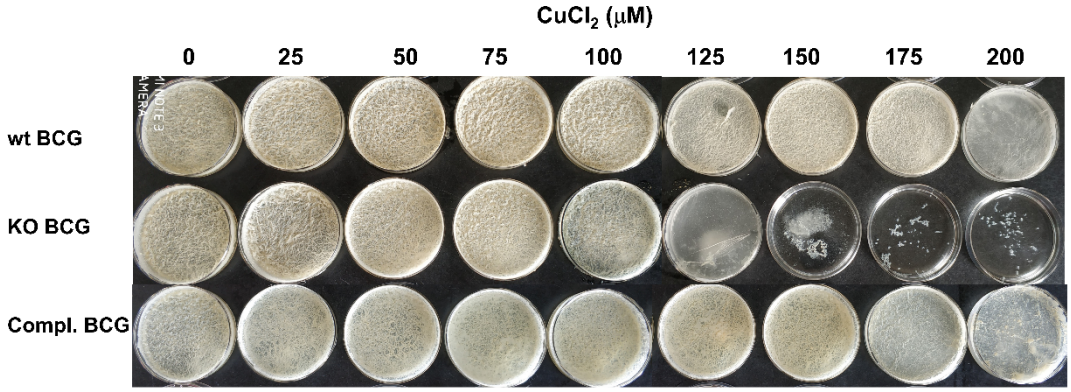

Figure 1. Impact of Cu^{2+} on biofilm formation of various *M. bovis* BCG strains. Wild type (wt), Δ*groEL1* (KO), KO complemented (compl.) *M. bovis* BCG strains grown in 3.5 % glycerol Sauton's medium in the absence or presence of various concentration $CuCl_2$ for three weeks. The figure is representative of at least three different experiments.

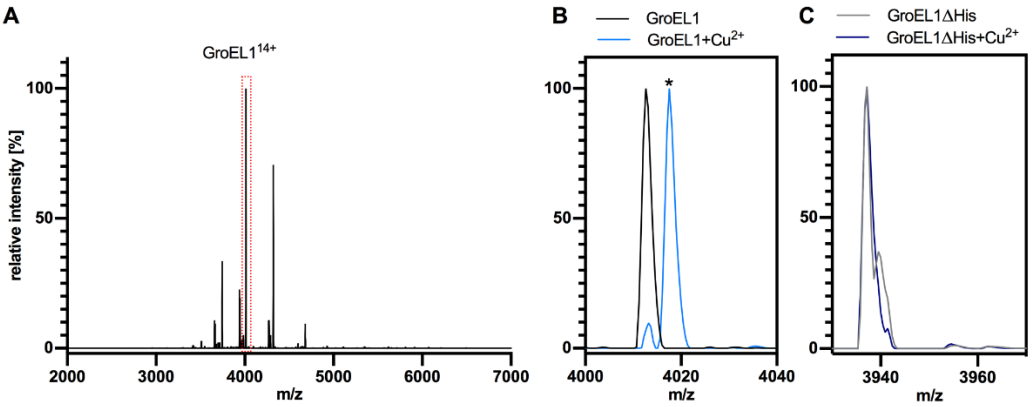

Figure 2. Native nano-ESI spectra of the GroEL1 and the GroEL1ΔHis variant showing different affinities for Cu^{2+}. The protein concentration was 7.5 µM in 500 mM ammonium acetate. (A) Full native mass spectrum of apo GroEL1 shows a narrow charge state distribution with the main charge state $[M + 14H]^{14+}$ highlighted in red. (B) Cu^{2+} binding to GroEL1 shown for the $GroEL1^{14+}$ charge state. A peak shift can be observed upon addition of an equimolar amount of Cu^{2+}, the peak for copper-bound GroEL1 is highlighted with an asterisk. (C) $GroEL1\Delta His^{14+}$ in the presence and absence of one molar equivalent of Cu^{2+}, showing no binding.

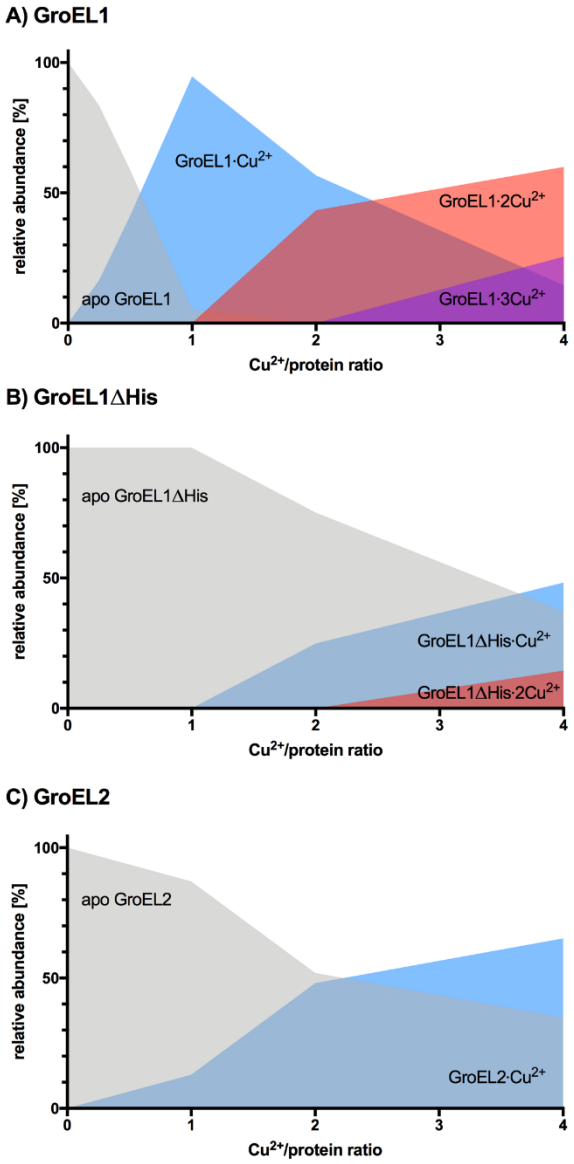

764

765 **Figure 3.** Relative abundance of the different protein-Cu adducts as determined
766 by native mass spectrometry. (A) GroEL1; (B) GroEL1ΔHis; (C) GroEL2. The
767 spectra were recorded at a final protein concentration of 7.5 μM in 500 mM
768 ammonium acetate. Grey, blue, red and purple areas indicate the abundance
769 of apo-protein, 1:1 complex, 2:1 complex and 3:1 complex of protein and Cu^{2+},
770 respectively. The titration with $CuCl_2$ was performed at molar ratios Cu^{2+} to
771 protein of 0.25:1, 0.5:1, 1:1, 2:1, and 4:1, corresponding to 1.9-30 μM $CuCl_2$.
772 Populations with < 5% intensity are not shown.

773

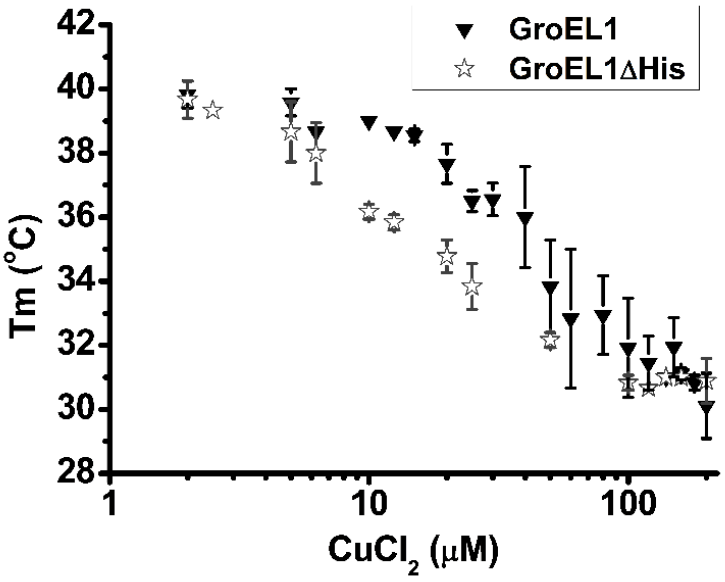

774

775 **Figure 4.** Thermal shift assay to analyse the effect of copper on GroEL1 protein
776 destabilization. The reaction (25 μL) contained 5 μM protein (GroEL1 or
777 GroEL1ΔHis), 0.3 μL of 5000 × SYPRO Orange, with various concentration of
778 $CuCl_2$ in 5 mM HEPES, pH 7.5. The data correspond to mean and standard
779 deviations and were obtained from three independent experiments.

780

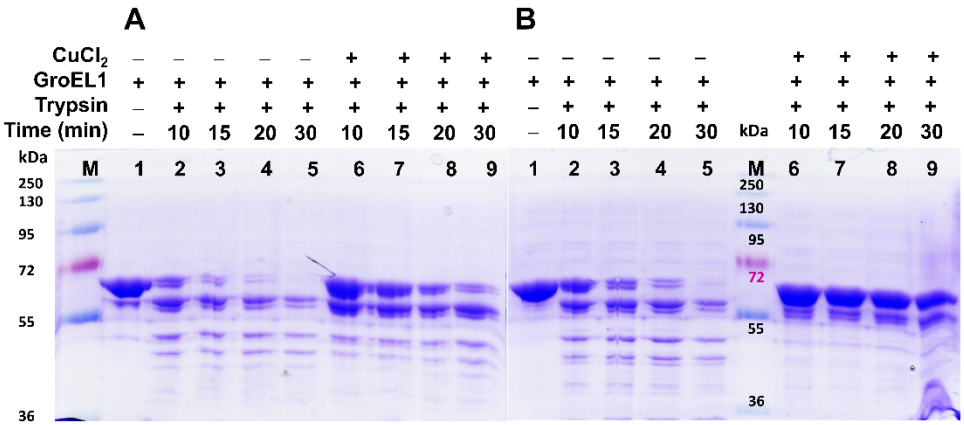

Figure 5. Limited trypsin digestion of GroEL1 (A) and GroEL1ΔHis (B) in the absence or the presence of Cu^{2+}. The reaction was stopped at different times (10, 15, 20, 30 min) by adding PMSF. The reaction products were analysed by 15% SDS-PAGE. Lane M: molecular mass standards; lane 1-9: 5 μg (~9 μM) of GroEL1 (or GroEL1ΔHis); lane 2 to 5: digestion for 10, 15, 20, 30 min, respectively, in the absence of Cu^{2+}; lane 6 to 9: digestion for 10, 15, 20, 30 min, respectively, in the presence of 18 μM Cu^{2+}. The figure is representative of three independent experiments.

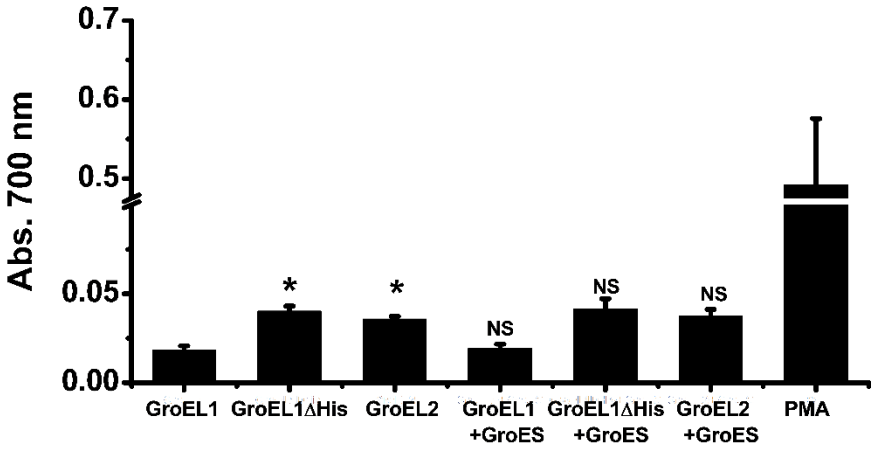

792

793 **Figure 6.** *M. tuberculosis* GroEL protein ATPase activity.

794 Enzymatic reactions were incubated with 10 μM GroEL and 20 μM GroES
795 proteins at 37 °C for 1 h and the absorbance was recorded at 700 nm. Plasma
796 membrane ATPase (PMA) was used as control. The mean from at least three
797 independent experiments for individual data sets was calculated and plotted
798 along with the standard deviation.

799

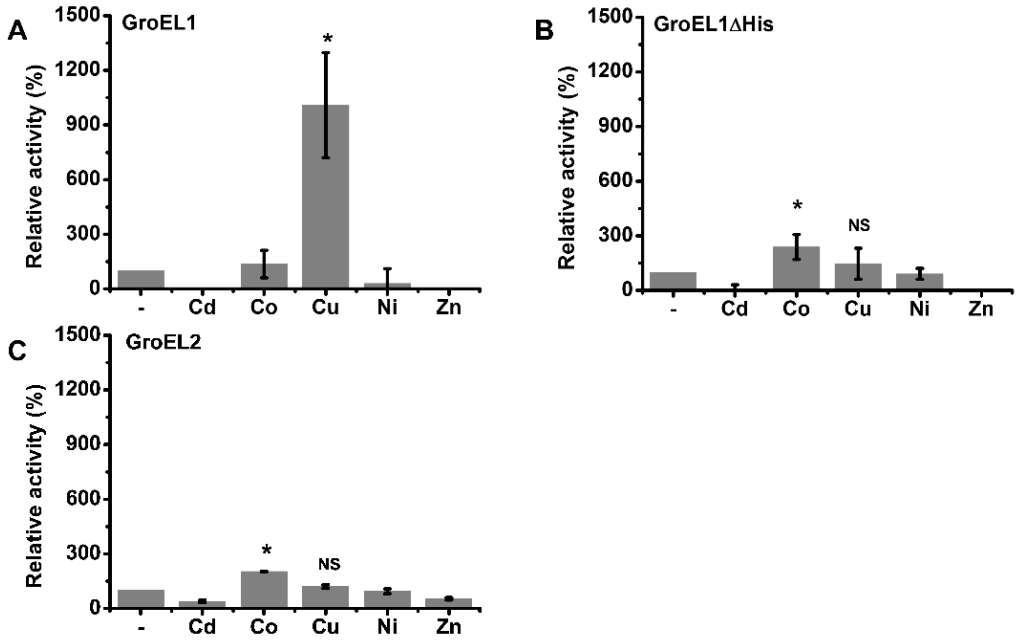

Figure 7. ATPase activity of 10 μM *M. tuberculosis* GroEL proteins in the presence of 100 μM metal ions. (A) GroEL1, (B) GroEL1ΔHis and (C) GroEL2. The mean from at least three independent experiments for individual data sets was calculated and plotted along with the standard deviation, considering the activity measured in the absence of metal ions as 100%.

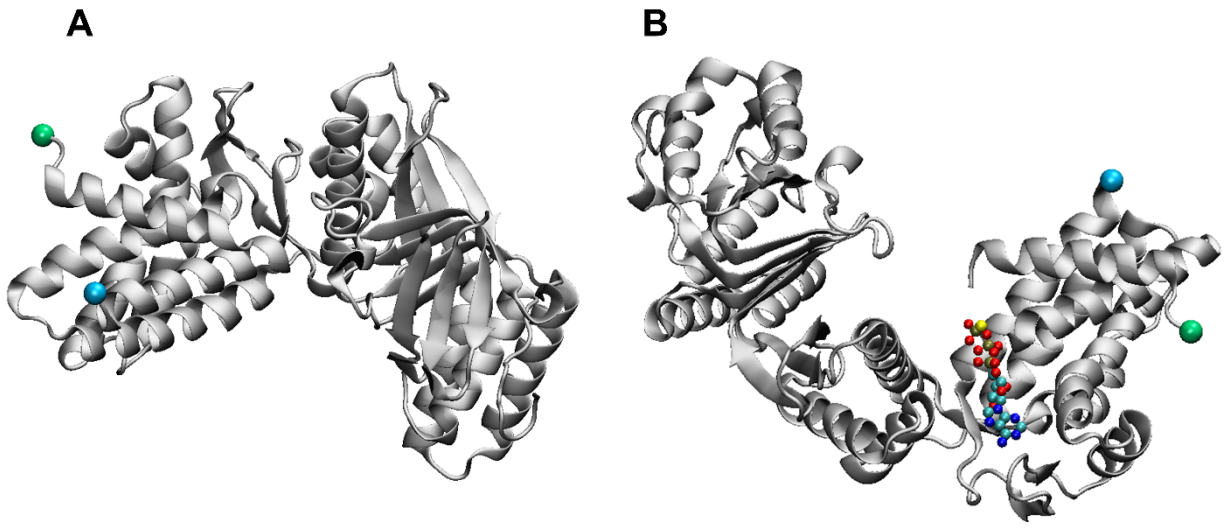

807

808 **Figure 8.** 3D model of GroEL1 represented as a silver cartoon without (A) or
809 with ATP analogue (B). The location of an ATP analog (ATPγS) results from the
810 superposition of the 3D model with the crystal structure of *E. coli* GroEL (PDB
811 ID: 1SX3). The Cα of the first (residue number 61) and last (residue 518) of the
812 model are shown as green and blue van der Waals spheres respectively.
813 [1]